DOI: 10.31276/VJSTE.64(2).86-94

Fabrication of electrospinner for producing tube-shaped artificial blood vessels toward treatment applications in cardiovascular diseases

Binh Thanh Vu[1, 2], Thai Minh Do[1, 2], Hiep Thi Nguyen[1, 2*]

[1]*School of Biomedical Engineering, International University, Ho Chi Minh city*
[2]*Vietnam National University, Ho Chi Minh city*

Received 5 April 2022; accepted 27 May 2022

Abstract:

One of the most common causes of high mortality in Vietnam, as well as in the world, is related to cardiovascular disease. Therefore, the development of artificial blood vessels to replace damaged blood vessels in cardiovascular patients has become increasingly necessary. Realizing a growing need for these techniques, our team manufactured a specialized electrospinner machine to produce artificial blood vessel models. The electrospinner has the following components: high power supply source, collectors with tubular-type structures, and a syringe pump system. This study was conducted to (i) fabricate electrospinner machine and (ii) operate and evaluate the electrospinner. We found that the conditions of vascular formation can be optimized and these influencing parameters include DC high voltage source, distance between needle tip and collector, needle tip diameter, speed of syringe pump, and ambient temperature and humidity. The results show that this equipment is stable and safe for users.

Keywords: **artificial blood vessel, cardiovascular diseases, electrospinner.**

Classification number: **3.6**

Introduction

Cardiovascular disease, including coronary artery disease and peripheral vascular disease, is the leading cause of death in Vietnam and other countries around the world. Therefore, the development of artificial blood vessels [1] to replace aging conduits in cardiovascular patients is becoming increasingly urgent, especially in bypass surgeries and other revascularization procedures. Tissue engineering offers the prospect of replacing damaged blood vessels. Recent advances in science have shown that it is possible to successfully replace human blood vessels. For example, cells can be grown into sheets of tissue to form a layer of vascular cells with impressive strength.

In recent years, electrospinning has revolutionized material science [2]. By this method, a solution (obtained by the melting or dissolution of one or a mixture of materials) is ejected into fibres ranging in size from micrometres to nanometres. A basic electrospinning device consists of three main parts: (i) a high voltage DC power supply that generates a steady voltage of several tens of kilovolts, (ii) a pump that controls the injection rate of the mentioned solution, and (iii) a grounded fibre collector [3]. The operation principle of electrospinning begins with using the force of an electric field to produce extremely thin fibres from a viscous solution, for example, a solution of polymers such as polycaprolactone [4], chitosan, polyvinyl alcohol, etc. These thin fibres follow the direction of the electric field force to the fibre collector and attach to it. When applying high voltage to the nozzle and grounding the fibre collector, there will be a large electric field between the nozzle and the collector. A very small current is generated, which electrifies the nozzle. Therefore, the solution passing through this nozzle is also electrified and the charged particles are accelerated by the electric field thereby ejecting the solution moving in the direction of the above electric field. As a result, the solution is uniformly accelerated and forms a thin filament with a radius as small as a few nanometres [5]. Currently, electrospinning is widely used on an industrial scale in various fields including electronics, semiconductors, environment, fashion, chemistry, and medicine and for

*Corresponding author: Email: nthiep@hcmiu.edu.vn

diverse applications as light-emitting diodes, kidney filters, and air filters [6].

With advancements in science and technology, electrospinning has also made great contributions to biomedical research in the manufacture of medical devices, especially in the fabrication of tissue scaffolds and controlled drug release systems [7]. Researchers around the world have been applying this method in their research to find innovative solutions for medical treatment. In Vietnam, the concept of electrospinning is quite new and has only been studied for the last five years. Currently in Vietnam there are only two research facilities that own (manufacture) electrospinning equipment: Hue University of Science and University of Technology, Vietnam National University, Ho Chi Minh city. Current market prices of electrospinning devices, including the cost to import to Vietnam, are about $20,000-500,000. Despite their excessive cost, the application ranges of the above devices are limited, especially in the context of artificial tissue manufacturing where interest in products used in the treatment of artificial skin and blood vessels continues to increase among domestic scientists.

The main components of an electrospinner include the high-voltage power supply, the syringe pump system, and the collector system as shown in Fig. 1. In the electrospinner, the machine's high voltage power supply is the core of the operation. This is a DC source that ranges from 5 to 30 kV. These power supplies on the market are expensive and are not suitable for our application. Therefore, we designed our own high voltage power supply. In addition, we designed a syringe pump system with a pumping speed of 1-20 ml/hour and plastic preformed structures for insulation purposes. The design of the fibre collector system is necessary to actively fabricate scaffolds of different shapes for applications in tissue engineering. The fibre collector was designed in the form of a hub to achieve a tubular structure. Then, we operated and assessed the electrospinner by fabricating tubular scaffolds and evaluating their surface structure.

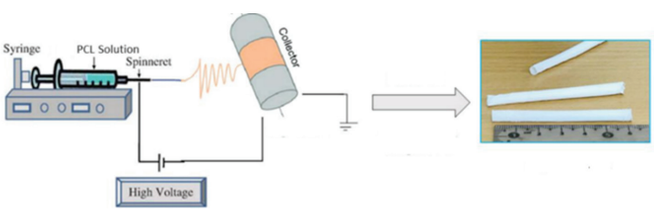

Fig. 1. Overview of the fabrication of polycaprolactone (PCL) tubes.

Materials and methods

Materials

Frozen bovine artery endothelial cells (BAECs) were provided by the School of Biomedical Engineering, International University, Vietnam National University, Ho Chi Minh city. BAECs were thawed and cultured in nutrient medium (DMEM, 10% foetal bovine serum, 1% antibiotics, Gibco) at 37°C, 5% CO_2 until 70-80% coverage of the culture dish was reached. Then, the BAECs were detached with Trypsin/EDTA 0.25% (Gibco) and seeded on PCL scaffolds to perform further evaluations.

Methods

Design of high voltage DC power supply:

From the 220 VAC main, the power source was rectified directly to a DC voltage of about 277 VDC via the use of a full power rectifier circuit. This high voltage DC source is then used as the power source for the DRIVER MOSFET, which opens and closes the FET at a very high frequency in the primary part of the flyback transformer. As a result, the output of the flyback transformer will be pushed to a very high DC voltage. This process is illustrated in Fig. 2.

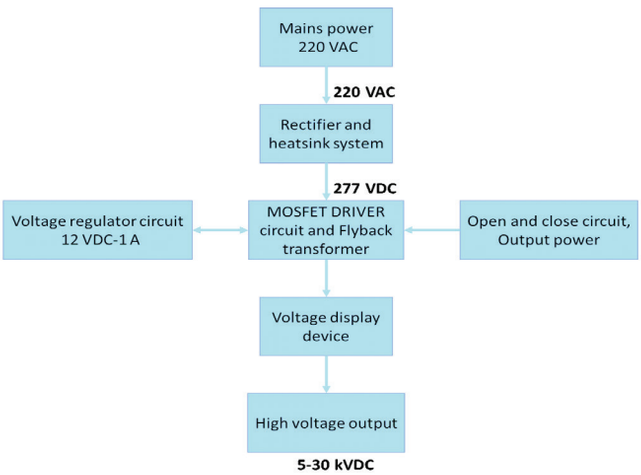

Fig. 2. High voltage DC power supply circuit block diagram.

The principle of operation of our designed electrical circuit is easy to understand and is also capable of solving interference problems. The circuit was designed on ORCAD software, which is a powerful software that supports electronic circuit design tasks. To simplify the circuit, the component pins are specifically labelled and marked with the power terminals, which helps engineers read and trace the design. The designed circuit is depicted in Fig. 3.

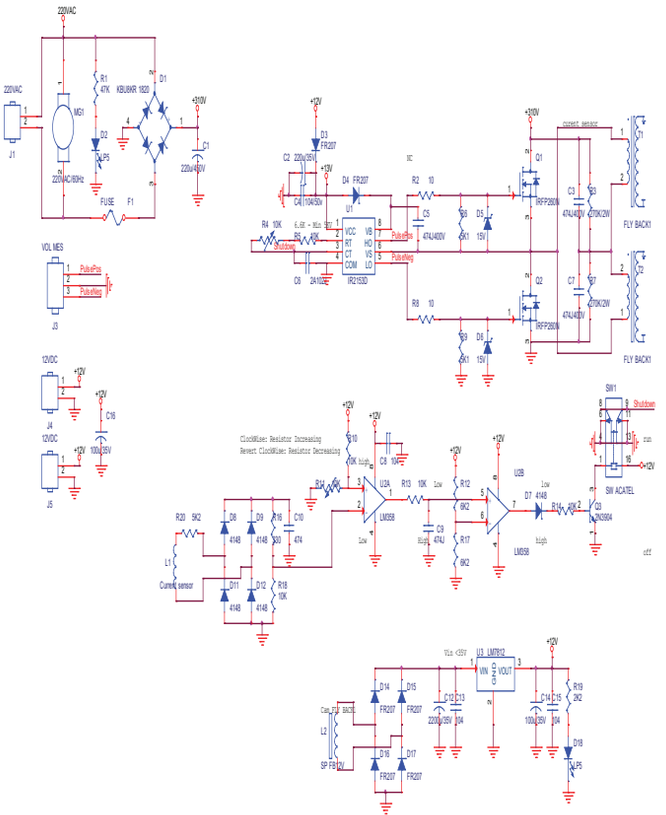

Fig. 3. The principal circuits of the high voltage source.

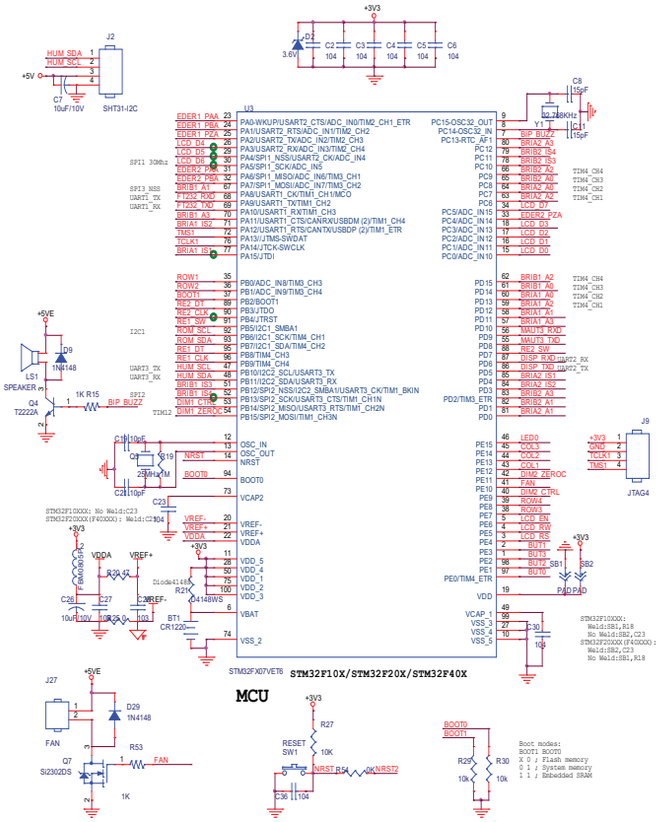

Fig. 4. Central control circuit of the collector system.

Design of fibre collector system:

The fibre collector system consists of one aluminium foil spool and one drum, which is a monolithic billet that is turned in a cylindrical shape. The system is rotated by a moving belt, which transmits the force from the motor to the shaft of the drum. The drum rotation is monitored by a microcontroller system.

The electronic circuit acts as the central processing task for the collector system. This circuit is designed with the central microcontroller ST32F407 with a core clock speed of 168 MHz, and support for processing 32-bit numbers. Therefore, it is suitable for motor control applications by PID algorithms. In addition, we also use specialized drivers for brushless motors to make control more convenient.

In this project, brushless motors are selected and used for its characteristics of large rotational power and low vibration at high speed as it is necessary to control and align the membranes (Fig. 4).

ZM-6405E brushless motor driver bridge: the DC motor driver ZM-6405E allows a large current supply, control over the brushless motor with a maximum power of 200 W and can accept PWM Analog signal voltage to control motor speed.

Brushless motor: the brushless motor BL75S10-230TF9 has a maximum power of 100 W at 3000 rpm and a force of 0.32 N.

Design of syringe pump system:

The syringe pump and slider system are controlled by the MCU slaver SMT32F030F4P6 as illustrated in Fig. 5. The main purpose of the master and slaver method is to stabilize the injection rate of the syringe pump in the range 0.1 to 20 ml/h with the cylinder sizes available on the Vietnamese market. Meanwhile, the slider system also needs to be controlled to move the syringe pump system back and forth.

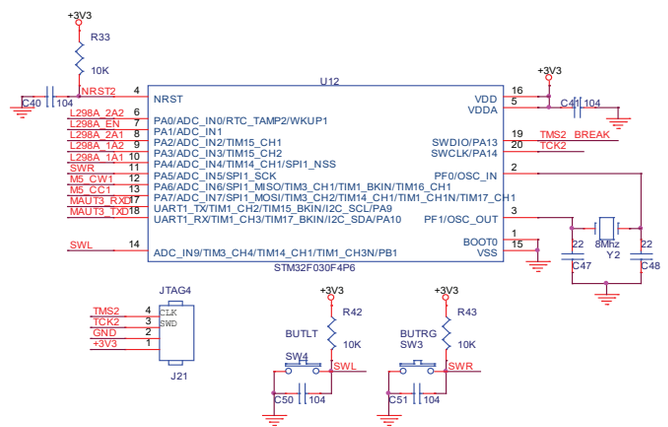

Fig. 5. The central control circuit of the syringe pump.

The needle and syringe system consists of two main components: a fixed frame (including two front shields to help hold the cylinder, two rear shields connecting the stepper motor, a 20x80-mm support frame made of fixed aluminium) and the moving part (including centre thrust plate, lead screw, nut and two-phase stepper motor). We use a screw mechanism to convert the circular motion of the stepper motor into the reciprocating motion of the cylinder. To limit the pushing speed to the maximum amount, we choose the lowest step screw bar of 1 mm combined with two round sliders mounted in parallel to support and balance the push cycle. Two linear bearings and screw nuts are rigidly fixed on the central thrust plate, which plays the role of fixing and transmitting the movement of the motor (Fig. 6).

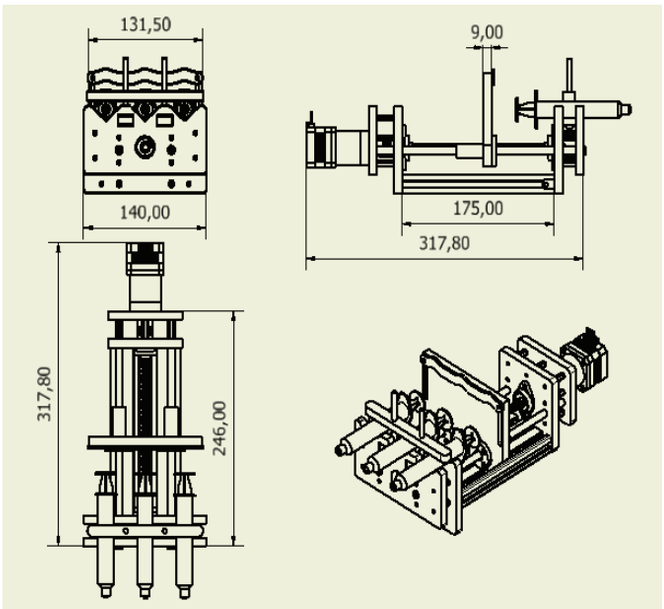

Fig. 6. Syringe pump system on Solidworks software.

PCL tubular fabrication:

The PCL tube is fabricated based on a long metal mould (4 cm length and 2, 3, or 4 mm diameter corresponding to the diameter of the tubular fibre collector) by electrospinning whose details are given below.

The electrospinning system consists of 1-3 piston(s) containing PCL solution and the nozzle is connected to the anode of the high voltage power source. On the other hand, the piston(s) is placed in a pump system with a pumping rate of 0.2 ml/h.

The collector is a metal mould shaft (4 cm length and 2, 3, or 4 mm diameter). The metal mould is connected to the cathode of the power supply and is stabilized in a rotating system with a speed of 750-800 rpm.

The procedure was carried out based on our previous study [8] and 15% PCL solution was prepared previously in acetone solvent.

- 5 ml of the solution is placed into the piston. The distance from the needle tip to the collector is set to 10 cm.

- The pumping system is set up with a pump rate of 0.2 ml/h.

- The high voltage power supply is 15-18 kV, and the collector has a rotation of 750-800 rpm.

- Electrospinning is done within 3-4 h to obtain a PCL tube.

Evaluate surface structure of PCL scaffold through Scanning electron microscope (SEM):

Scanning electron microscopy (SEM) can produce high-resolution images of a specimen by using a narrow beam of electrons scanning the surface of a specimen, which is followed by the recording and analysis of the radiation emitted from the interaction of the electron beams with the sample surface to obtain an image of the specimen with high magnification.

Evaluate BAEC adhesion and proliferation on PCL scaffold through SEM:

- Use a 1-ml needle to transfer the BAEC suspension onto the PCL scaffolds in a 96-well plate, which was then supplemented with culture medium and placed in the humidified incubator.

- After defined time intervals, samples were washed three times (1-2 ml each time) with phosphate-buffered saline (PBS).

- The sample was then soaked in 2.5% glutaraldehyde at 4^{o}C for 2 h.

- Remove excess glutaraldehyde solution, wash with PBS 2-3 times.

- Samples are soaked in alcohol at 30^{o}, 50^{o}, 75^{o} and 96^{o}, respectively, for 20 min each time. The sample was then allowed to dry at room temperature.

- Conduct SEM.

Results and discussion

Design of high voltage DC power supply

In this study, we designed an 11x15-cm PCB board using FR4 material with two layout layers. This printed circuit was designed with multiple lines with a large width to ensure the power of the power supply is operated efficiently. This motherboard is shown in Fig. 7. In addition, we also designed a display PCB main that indirectly measures high voltage from the primary source signals as illustrated in Fig. 8.

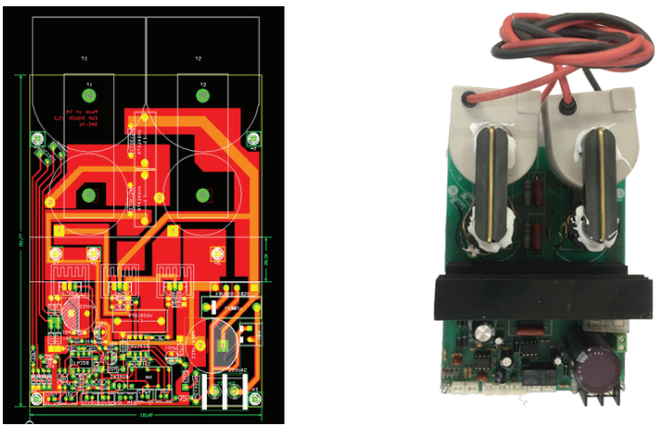

Fig. 7. Layout of the high voltage power supply circuit.

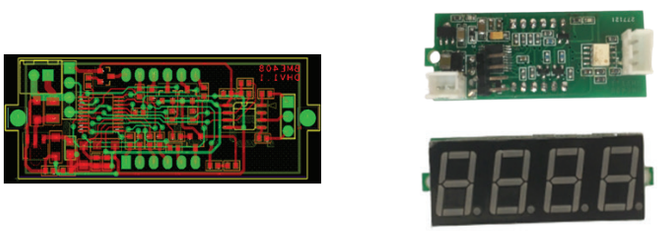

Fig. 8. High voltage display circuit.

To prevent electromagnetic interference in a high voltage field, the power supply was completed with aluminium housing. We reviewed several power supplies on the market and produced an optimal solution that makes the high-voltage power supply easy to use and safe. It was designed with a power switch, display of the output voltage status, and a single knob to adjust the output voltage. In addition, it also has a built-in display of current and voltage. The completed power supply is shown in Fig. 9.

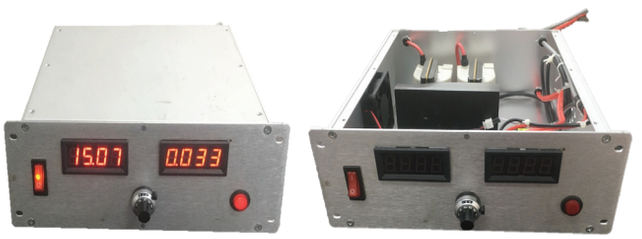

Fig. 9. DC high voltage power supply after being successfully built.

A crucial factor when researching, manufacturing, and operating high voltage power supplies is safety assurance. To avoid fatal injuries caused by high voltage, the grounding part of the high voltage system should be managed with care. Do not operate a high voltage power supply system without grounded wiring. The user needs to ensure a minimum distance from the high voltage electrodes. When voltage is being supplied, a retention distance of at least ½ inch per kV is recommended [9]. In addition, it is necessary to maintain dry conditions and provide insulating boots to the user if necessary. Several distances are calculated as follows:

100 kV → 100 x (2.54/2) = 100 x 1.27 = 127 cm = 1.27 m

50 kV → 0.635 m

30 kV → 38.1 cm

Design of fibre collector system

We used ORCAD Layout software to design the PCB. The central processor STM32F407 was designed in the middle of the main, while other power components such as the H-bridge and the source are mounted with heat sinks and placed on the outside to reduce temperature during operation. The PCB layout circuit is illustrated in Fig. 10.

The MCU enters the corresponding task segments to increase or decrease the target value, and thanks to the PID algorithm, the actual rotation speed asymptotically follows the desired value.

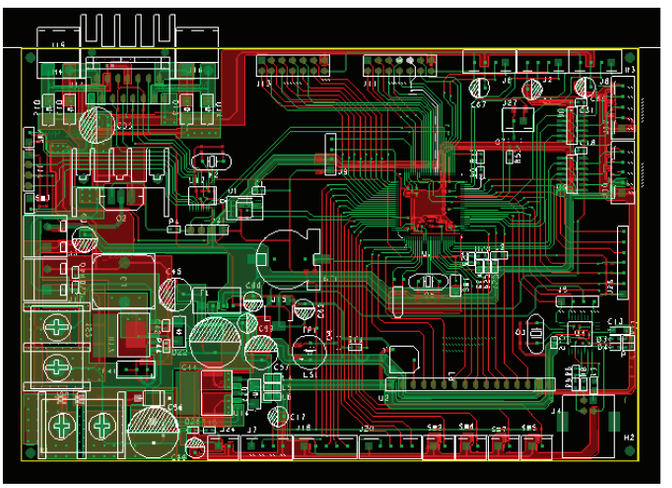

Fig. 10. PCB main control of the collector system.

Upon entering the program, the microcontroller initializes peripherals such as H-bridge, EEPROM, and LCD display by sending data frames to the display device. Next, the central controller loads the default values for these peripherals set in the EEPROM. PID, timer, and H-bridge parameters are initialized. This motor control process is based on a PID algorithm with pulse feedback inputs read from the encoder to record the round(s) per minute. The actual rotation speed approaches the desired value thanks to the control algorithm. The interplay between two microcontrollers on the main, MCU Master STM32F407, and MCU slave for slider and syringe pump function uses UART interrupts.

The collector control system was installed in an aluminium box to prevent electromagnetic interference

from the external high-voltage field (Fig. 11). The LCD used is a 20x4 type that can display not only collector control information but also other information such as infrared light, syringe pump, humidity, and temperature. Interactions with user will be via 3 x 4 matrix pushbuttons and knob encoder.

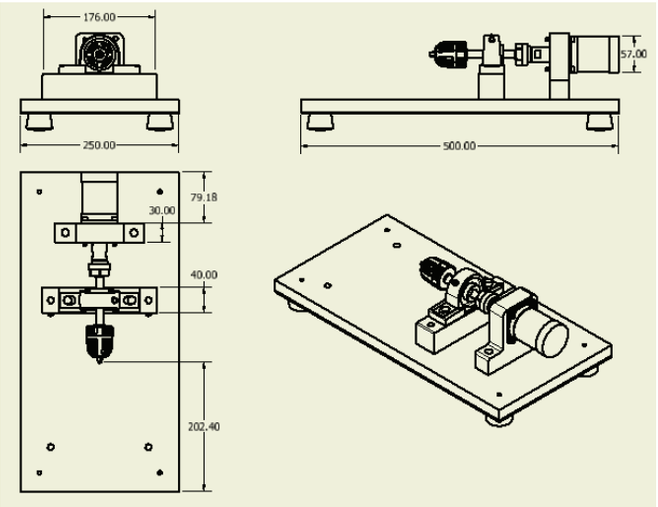

Fig. 11. Design of the mandrel collector system.

Syringe pump system design

The TB6600 stepper motor driver circuit uses the IC TB6600HQ/HG is used for stepper motors 42/57/86 that is either 2-phase or 4-wire with load current of 4A/42VDC, which is commonly applied in machines such as CNC, laser, or other automatic machines (Fig. 12). Measure is a dedicated control bridge for the stepper motor, which will make the syringe pump control easier and more accurate.

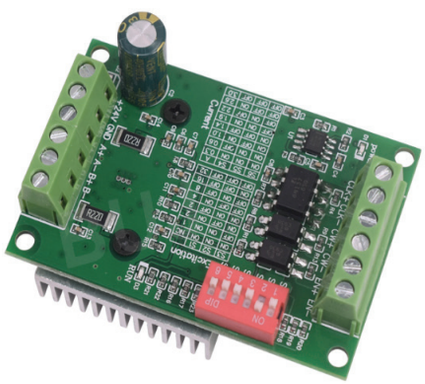

Fig. 12. Stepper motor driver bridge TB6600.

When the system starts, the master microcontroller will send a command to the slaver processor of the syringe pump system to initiate the command according to the parameters set in the ROM. The slaver processor will initiate the pump speed and move the slider.

In the main processing loop, the slaver processor will wait for a command from the master processor. If an instruction is received via the UART interrupt, the processor immediately executes that instruction. When complete, the processor will stop pumping and move the slider back to its original position.

Calculation of pump speed, travel speed, and slider movement range are also performed in by program in the slaver MCU.

With the need to create greater polymer coverage on the mandrel, we use a slider system driven by a 4-phase stepper motor that combines with the syringe pump system. The system is programmed to generate a cyclic motion over a fixed distance through the lead screw system and the slider. On the slider, there are several available positions to fix the needle pump, which makes it easy to adjust the distance between the needle and collector (Fig. 13). The system will automatically align the distance on the slider thanks to a travel switch placed in the original position of the coordinates.

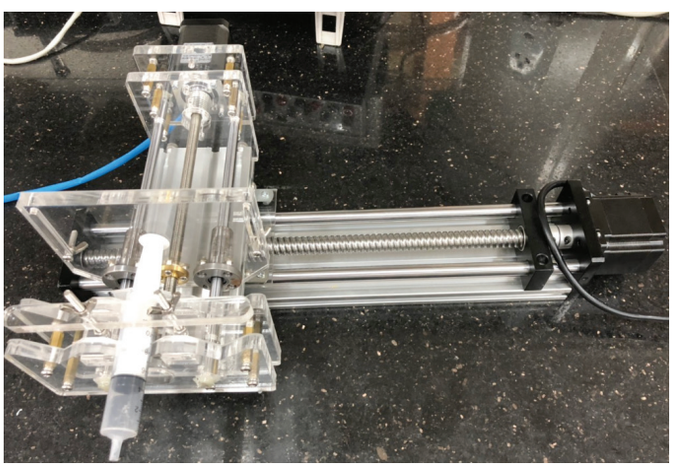

Fig. 13. Syringe pump system installed on the slider.

Fabrication of tubular Polycaprolactone (PCL) scaffold

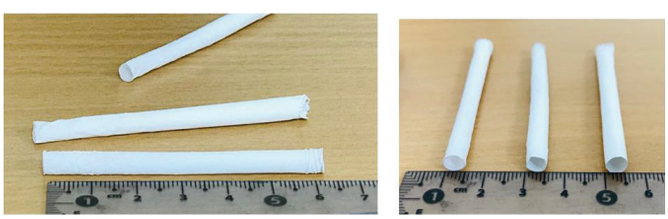

Fig. 14. Macroscopic structure of PCL tubes.

Figure 14 shows the macroscopic structure of the PCL tube obtained after being fabricated by electrospinning i.e., ejecting the polycaprolactone solution in a high-

voltage electric field). After using this method, the obtained scaffold has an average length of 4-5 cm and diameter of 2, 3, or 4 mm based on the shape of the collector mould.

Surface structure of PCL scaffold

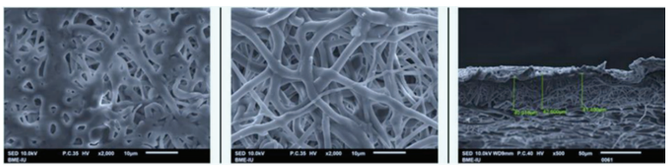

Fig. 15. The microstructure of the PCL tube fabricated by electrospinning. The measured thicknesses are 40.018, 42.000, and 41.400 µm, respectively.

After using electrospinning to obtain a tubular structure similar to blood vessel, the microstructure was observed by SEM as depicted in Fig. 15. Under high magnification (x2000), the structure of the PCL scaffold is made up of micrometre-sized filaments on both the inner and outer surfaces. However, the shapes of the inner and outer surfaces of the PCL tube are different. The inner fibres have more of a flat shape than the outer fibres. This is explained by the fact that the inner surface is in direct contact with the collector during electrospinning and the charged fibres/particles of the PCL solution move from the needle tip to the collector at a certain speed. Finally, the fibres/particles hit the collector, which causes the polymer fibres in the innermost layer (inner surface) to have a flat shape compared to the outer surface.

According to the descriptions of the structural types of blood vessels, the diameter varies depending on vascular classifications along with other factors such as anticoagulation capacity, mechanical durability, etc. Of which, the ability to prevent blood clotting is one of the most important prerequisite properties of blood vessels in general. This ability, according to previous studies, comes from secreted proteins of the monolayer of endothelial cells in the lumen of the vessel.

A dense structure of PCL fibres stacked and interlaced form a small pore structure that makes it difficult for cells to penetrate deep into the inner structure of the PCL tubule. This structure readily forms monolayers of endothelial cells.

In addition, in Fig 15, the thickness of the PCL tube was recorded at high magnification, which was found to be around 40-42 µm. This thickness, along with the physical properties of PCL, creates a conduit structure bearing the appropriate properties as well as a certain elasticity. This data has been published in our previous studies that show suitability for making artificial blood vessels.

Thus, this study has fabricated PCL scaffolds with basic characteristics of small vascular tubes: diameters of 2, 3, or 4 mm, physical-mechanical strength, and a structure that facilitates a monolayer of endothelial cells established within the lumen of the vessel.

Spreading ability of BAECs on PCL tubes

After determining the stable BAEC cell line through subcultures, cells were examined for their ability to spread on the PCL structure. Fig. 16 depicts the interaction of BAECs on PCL scaffolds based on images of the cell shape and extracellular matrix (ECM) region, which were taken on day five of culture.

In the absence of cells (Fig. 16A), the inner surface of the tube is composed of a structure of randomly arranged and stacked micrometre-sized fibres (a consequence of the electric field due to electrospinning) followed by a very small pore structure of irregular shape. In general, the scaffold structure is uneven but still has stability in fibre size, structure, and pore size fluctuations of about 1-3 µm. Because it is composed of microfibers, the surface of the scaffold structure has a relative roughness, which is one of the factors that facilitates cells adherence to the PCL substrate.

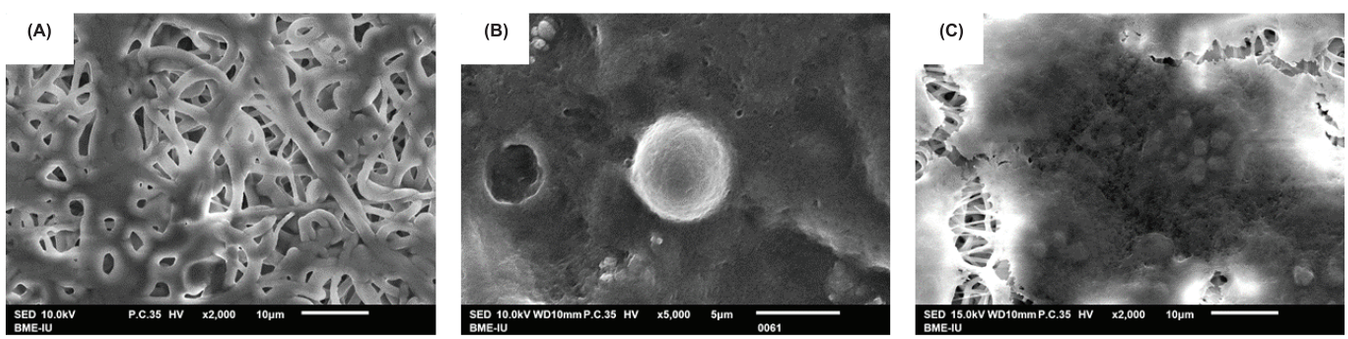

Fig. 16. Interaction of BAECs on PCL scaffolds. (A) The inner surface of the PCL matrix is devoid of cells. **(B)** BAECs at day five of culture on PCL scaffold. **(C)** The extracellular matrix region of BAECs at day five of culture on PCL scaffold.

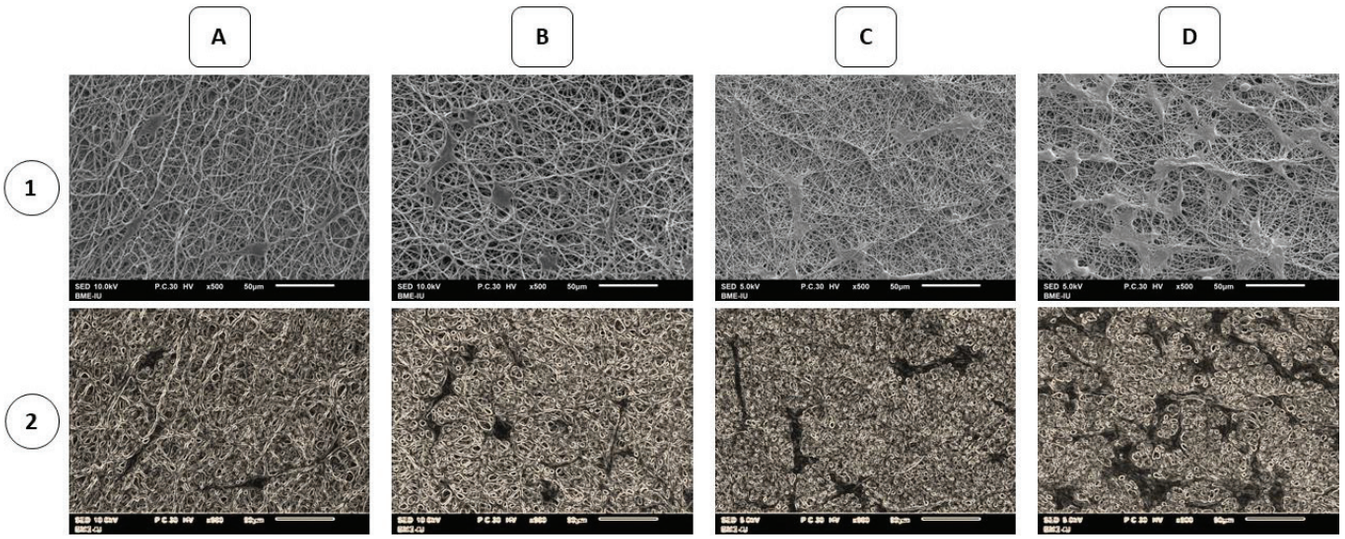

Fig. 17. The proliferation ability of BAECs on PCL scaffold. BAECs on PCL scaffold after **(A)** 1, **(B)** 2, **(C)** 3, and **(D)** 4 d of culture.

Figure 16B shows the cells in the process of spreading onto the attachment surface. At this point, the cell has a rounded tip and the surrounding part begins to spread and mix with the ECM, which is secreted by the cell itself and neighbouring cells. Here, the boundary between the cell and the ECM is indistinguishable. One of the features that helps us see the attachment site of the cell is that the cell-ECM structure hides the underlying matrix and the fibrous structure and voids are gone.

The SEM image in Fig. 16C shows that the substrate is rough and slimy. Between them, there are small grooves consisting of zigzag lines that cross each other. This is one of the demonstrations showing the compatibility of PCL for animal cells in general, or bovine artery endothelial cells - the main subject of this study.

Proliferation of BAECs on PCL scaffold

SEM images were recorded through days 1, 2, 3 and 5 (Fig. 17-1), and the image shows that the cells spread on the scaffold increase in density over time. SEM images were contrast processed in Microsoft PowerPoint to increase the prominence of cells on the substrate (Fig. 17-2). On day 1 (Fig. 17A), the cells spread in very small numbers. Cells retained their elongated, dendritic shape on subsequent observation days (Figs. 17B, 17C, and 17D).

The results showed that the adhesion and proliferation of BAECs on PCL scaffolds were highly effective. Over the culture period, cells adhered evenly to the surface of the scaffold structure. On the other hand, the cell's ability to attach to the scaffold was highly influenced by the pore size of the scaffold and by the binding between receptors and ligands.

The above results showed that *in vitro* cultures of BAECs on PCL scaffolds do not cause changes to the structure of the scaffold and the data portrays stable spread and proliferation of this cell line. These outcomes suggest the possibility that PCL scaffolds can be used for long-term *in vitro* culture.

Conclusions

We designed and fabricated the basic components of an electrospinner. Of these components, a variable high voltage DC power supply that ranges between 5 kVDC and 30 kVDC with display of current and voltage was constructed. Second, a collector system (mandrel) that ejects polymer fibres out of a solution and evaporates solvents to fabricate PCL scaffolds, which are the structure that facilitates cell attachment and growth to develop artificial blood vessels. Finally, the syringe pump system that integrates three needles on the system and an integrated reciprocating mechanism to increase the homogenous coverage of the nanofibers on the collectors. Electrical designs were developed on ORCAD software, mechanical designs were developed on SOLIDWORKS, INVENTOR software. These programs make it easier for engineers to calibrate and develop versions of the machine later.

Given the heat-sensitive characteristics of medical synthetic polymers (i.e., the low melting point of 60^{o}C for PCL), the process of fabricating polymer fibres by electrospinning should not cause fibre fractures or changes in chemical or crystal structure by manipulation at room temperature. Therefore, in the fibre forming process, the polymer is mixed in organic solvents at a temperature lower than the melting point (50^{o}C). The

solvents used for dissolution are highly volatile solvents, so the polymer fibres will almost immediately dry when collected at the collector at room temperature. The *in vitro* results of BAEC cultures on PCL tubes fabricated from our electrospinner showed that the cells exhibited excellent spreading and proliferative ability over time, which demonstrated that our electrospinning PCL tubes exhibit promising cytocompatibility.

ACKNOWLEDGEMENTS

This research was funded by Vietnam National University, Ho Chi Minh city (VNU-HCM) under grant number C2020-28-08.

COMPETING INTERESTS

The authors declare that there is no conflict of interest regarding the publication of this article.

REFERENCES

[1] E.C. Filipe, et al. (2018), "Rapid endothelialization of off-the-shelf small diameter silk vascular grafts", *JACC: Basic to Translational Science*, **3(1)**, pp.38-53.

[2] Z.M. Huang, et al. (2003), "A review on polymer nanofibers by electrospinning and their applications in nanocomposites", *Composites Science and Technology*, **63(15)**, pp.2223-2253.

[3] D. Li, Y. Xia (2004), "Electrospinning of nanofibers: reinventing the wheel?", *Advanced Materials*, **16(14)**, pp.1151-1170.

[4] N. Tran, et al. (2020), "Polyurethane/polycaprolactone membrane grafted with conjugated linoleic acid for artificial vascular graft application", *Science and Technology of Advanced Materials*, **21(1)**, pp.56-66.

[5] D. Lukas, et al. (2009), "Physical principles of electrospinning (electrospinning as a nano-scale technology of the twenty-first century)", *Textile Progress*, **41**, pp.59-140.

[6] S. Ramakrishna, et al. (2006), "Electrospun nanofibers: solving global issues", *Materials Today*, **9(3)**, pp.40-50.

[7] N. Zhu, X. Chen (2013), "Biofabrication of tissue scaffolds", *Advances in Biomaterials Science and Biomedical Applications*, IntechOpen, DOI: 10.5772/54125.

[8] N.M.P. Tran, et al. (2020), "Conjugated linoleic acid grafting improved hemocompatibility of the polycaprolactone electrospun membrane", *International Journal of Polymer Science*, **2020**, DOI: 10.1155/2020/8127570.

[9] ViTREK 4700 Operating and Maintenance manual 2018, vitrek.com/downloads/4700/4700_Operating_Manual.pdf, 55pp.